Available online at www.sciencedirect.com
SCIENCE DIRECT®
Journal of Sound and Vibration 293 (2006) 171–195
JOURNAL OF SOUND AND VIBRATION
www.elsevier.com/locate/jsvi

# Analysis and design of passive low-pass filter-type vibration isolators considering stiffness and mass limitations

C. Yilmaz*, N. Kikuchi

*Department of Mechanical Engineering, University of Michigan, Ann Arbor, MI 48109, USA*

Received 2 May 2005; received in revised form 23 August 2005; accepted 28 September 2005
Available online 10 November 2005

**Abstract**

The aim of this paper is to design stiff and lightweight uniaxial passive vibration isolators that have low stop-band frequency. In order to make fair comparisons, stop-band frequencies of various isolator designs are formulated in a general framework. Two new $n$-degree-of-freedom ($n$-dof) isolator designs are introduced. The first design has $n-1$ anti-resonance frequencies (zeros), which are generated by $n-1$ single-degree-of-freedom (sdof) dynamic vibration absorbers (DVAs). It is shown that this system offers lower stop-band frequency than an equivalent mass–spring chain, which just uses resonance frequencies to achieve isolation. The second design is synthesized using $n$ lever-type anti-resonant vibration isolators in series, so it has $n$ zeros. It is shown that this design attains lowest stop-band frequency when all the isolator mass is concentrated on lever tips. Finally, comparative numerical examples are presented.


## 1. Introduction

This paper is about undamped uniaxial low-pass filter-type vibration isolators used in the case of harmonic base excitation. The term "low-pass filter" is used to emphasize that all the isolator designs in this paper achieve isolation only after some frequency known as stop-band frequency. One of the challenges in passive vibration isolation is to obtain low stop-band frequency given a lower bound on isolator stiffness and an upper bound on isolator mass. If there is no lower bound on the isolator stiffness, a spring with the lowest possible stiffness can yield a very low stop-band frequency. However, for most applications there is a minimum stiffness requirement and a simple spring may not provide a low enough stop-band frequency. In order to solve the low stiffness problem by passive means, sometimes the object (load) that is to be protected is fastened to a massive structure (inertia block), which is in turn supported on stiff isolators. To increase the stiffness of the isolators substantially, one should use huge inertia blocks. This method is used in force isolation of stationary diesel engines or forging presses [1]. It is also used in seismic isolation of sensitive instruments. However, for most applications this method violates a mass constraint.

So far only single-degree-of-freedom (sdof) vibration isolation systems are considered. For sdof undamped passive vibration isolation systems, transmissibility is proportional to $1/\omega^2$, provided that the excitation

*Corresponding author. Tel.: +1 734 936 2926; fax: +1 734 647 3170.
*E-mail addresses:* cyilmaz@umich.edu (C. Yilmaz), kikuchi@umich.edu (N. Kikuchi).

0022-460X/$ - see front matter © 2005 Elsevier Ltd. All rights reserved.
doi:10.1016/j.jsv.2005.09.016

**Nomenclature**

| | |
|---|---|
| AMD | auxiliary mass damper |
| DAVI | dynamic anti-resonant vibration isolator |
| DVA | dynamic vibration absorber |
| $\mathbf{F}$ | forcing vector |
| HEM | hydraulic engine mount |
| $k$ | overall stiffness of an isolation system from the base to the load |
| $k_i$ | stiffness of the $i$th spring in an isolator |
| $k_i^a$ | stiffness of the $i$th absorber spring in the case of DVA equipped springs |
| $\mathbf{K}$ | stiffness matrix |
| $l_1$ | length of the lever in the case of single-degree-of-freedom lever-type anti-resonant vibration isolators |
| $l_2$ | distance between two pivot points in the case of single-degree-of-freedom lever-type anti-resonant vibration isolators |
| $m$ | load mass |
| $m_i$ | $i$th absorber or isolator mass |
| $m_i^S$ | mass of the $i$th stage in a multi-degree-of-freedom lever-type anti-resonant vibration isolator |
| $m_{\text{is}}$ | total mass of the isolator |
| $\mathbf{M}$ | mass matrix |
| mdof | multi-degree-of-freedom |
| $r$ | normalized excitation frequency |
| $r_{ws}$ | normalized stop-band frequency of a single-degree-of-freedom mass–spring system |
| $r_{ws}^{\text{in}}$ | normalized stop-band frequency of a single-degree-of-freedom mass–spring system with inertia block |
| $r_{ws}^{\text{op}}$ | normalized stop-band frequency of a 2-degree-of-freedom Type II optimum design |
| $r_{ws}^I$ | normalized stop-band frequency of a Type I anti-resonant vibration isolator |
| $r_{ws}^{II}$ | normalized stop-band frequency of a Type II anti-resonant vibration isolator |
| $R_{rws}$ | ratio of the normalized stop-band frequency of a 2-degree-of-freedom Type II optimum design to normalized stop-band frequency of an equivalent Type II anti-resonant vibration isolator |
| sdof | single-degree-of-freedom |
| $T(\omega)$ | transmissibility |
| $T_0$ | maximum allowable transmissibility in the stop-band |
| $x$ | displacement of load |
| $x_i$ | displacement of the upper end of the $i$th isolator spring in a multi-degree-of-freedom isolation system |
| $X$ | displacement amplitude of load |
| $\mathbf{X}$ | displacement vector |
| $y$ | displacement of base |
| $Y$ | displacement amplitude of base |
| $z$ | displacement of the isolator mass in the case of single-degree-of-freedom lever-type anti-resonant vibration isolators |
| $z_i$ | displacement of the $i$th absorber mass in dynamic vibration absorber equipped springs |
| $\alpha$ | lever ratio in single-degree-of-freedom lever-type anti-resonant vibration isolators |
| $\alpha_i$ | lever ratio of the $i$th isolator in a multi-degree-of-freedom lever-type anti-resonant vibration isolator |
| $\mu$ | ratio of isolator or absorber mass to load mass |
| $\omega$ | excitation frequency |
| $\omega_p$ | resonance frequency (pole) of a system having a single pole |
| $\omega_{pi}$ | $i$th resonance frequency (pole) |
| $\omega_{\text{peak}}^i$ | $i$th local peak frequency in the transmissibility plot of a multi-degree-of-freedom anti-resonant vibration isolator |
| $\omega_s$ | stop-band frequency of a single-degree-of-freedom mass–spring system |
| $\omega_s^{\text{ch}}$ | stop-band frequency of a multi-degree-of-freedom mass–spring chain |
| $\omega_s^{\text{dva}}$ | stop-band frequency of a dynamic vibration absorber equipped spring isolation system |
| $\omega_s^{\text{in}}$ | stop-band frequency of a single-degree-of-freedom mass–spring system with inertia block |
| $\omega_s^I$ | stop-band frequency of a Type I anti-resonant vibration isolator |
| $\omega_s^{II}$ | stop-band frequency of a Type II anti-resonant vibration isolator |
| $\omega_z$ | anti-resonance frequency (zero) of a system having a single zero |
| $\omega_{zi}$ | $i$th anti-resonance frequency (zero) |
| $\omega_0$ | natural frequency of a single-degree-of-freedom mass–spring system with mass $m$ and stiffness $k$ |

frequency, $\omega$, is much larger than the resonance frequency of the system. However, in an $n$-degree-of-freedom ($n$-dof) uniaxial mass–spring chain, transmissibility is proportional to $1/\omega^{2n}$, for frequencies much larger than the highest resonance frequency. Therefore, the attenuation rate can be increased by introducing additional masses to the isolation system. Without a mass constraint, a multi-degree-of-freedom (mdof) system can have a lower stop-band frequency than an equivalently stiff sdof system. Moreover, additional degrees of freedom provide better attenuation. These kinds of isolators are used in gravitational wave detection systems [2,3]. However, if there is a reasonable constraint on the isolator mass, then the highest resonance frequency of a mdof system will be much higher than of an equivalently stiff sdof system. Consequently, unless the transmissibility requirement is very small, the stop-band frequency of a mdof system will be much higher than that of an equivalently stiff sdof system. In order to lower the stop-band frequency to the level of the simple sdof system, stiffness should be lowered considerably. Please refer to Brillouin [4] and Winterflood [2] for more information on mdof mass–spring chains.

All the previously mentioned isolator designs just use resonance frequencies to achieve isolation. There are also low-pass electrical filters (LC filters) just based on resonance frequencies, e.g. Bessel, Butterworth or Chebyshev filters. However, elliptic (Cauer) filters are different from the aforementioned filters. These filters utilize anti-resonance frequencies (zeros) besides resonance frequencies (poles). When compared to the other low-pass LC filters, elliptic filters offer sharper attenuation response [5,6]. Fortunately, there are passive vibration isolator designs that make use of anti-resonance frequencies. In a linear lumped parameter system, anti-resonance frequencies can be generated by two different methods. The first method is to add dynamic vibration absorbers (DVAs). The second method is to generate inertial coupling.

DVAs were introduced by Frahm [7] in the beginning of the 20th century. A sdof DVA basically consists of a mass supported by an undamped spring (similar systems with damping are called auxiliary mass dampers (AMDs) and these systems are used for reducing amplification but not for isolation [8]). DVAs are generally used for isolating discrete frequencies. Hence, they may be listed under the title ''band-stop filter-type vibration isolators''. They are sometimes attached to uniaxial mass–spring chains in order to generate anti-resonance frequencies [9,10]. However, that configuration cannot be used in low-pass filter-type applications due to additional resonance frequencies generated by the DVAs spoiling the required pole-zero order. Although not mentioned frequently, DVAs have the potential to form low-pass filters in a different configuration. This potential will be utilized in this paper to form vibration isolators that can outperform resonance-only mass–spring chains.

Vibration isolators that utilize inertial coupling to generate anti-resonance frequencies were first developed in the 1960s by researchers in the aerospace industry for both band-stop and low-pass filter-type applications. The development of a new kind of vibration isolator was due to strict requirements on stiffness and mass of the isolators used in the aerospace industry. Flannelly [11] called this new system a dynamic anti-resonant vibration isolator (DAVI). DAVI uses a levered mass–spring combination to generate an anti-resonance frequency (zero) in the system. Anti-resonance occurs when the inertial force generated by the levered mass cancels the spring force. This happens at a particular frequency, which depends on the mass of the isolator, the lever ratio and the spring stiffness. Unlike DVAs, DAVIs are implemented on the load path; therefore the dof of the system is not increased. Furthermore, when a DAVI is introduced to a sdof system, inertial forces generated by the levered mass increases the effective mass of the system. Thus, the resonance frequency decreases and the isolator is capable of operating in a lower-frequency range. For applications in the aerospace industry, please refer to Rita et al. [12], Braun [13,14], Desjardins [15], Desjardins and Hooper [16]. Moreover, Ivovich and Savovich [17] show an application of this system for reduction of low frequency excitations transmitted from machines to their floor supports.

The lever in a DAVI amplifies the motion of a small mass, which in turn generates large inertial forces. This inertial amplification can be achieved by various methods. See Rivin [18] for a system that uses a flywheel and a ball screw having a small helix angle. Also see Goodwin [19] and Halwes [20] for systems that utilize hydraulic leverage instead of mechanical leverage. Fluid-type systems can provide higher leverage than the mechanical ones. Thus, a small mass of a fluid could generate the desired inertial forces, enabling weight savings on the system. For more information please refer to Braun [13,14], Smith and Redinger [21], and McGuire [22].

In the automotive industry, a similar kind of isolator was introduced in the 1980s to replace the rubber engine mounts that do not offer much control on damping and stiffness. Corcoran and Ticks [23], and Flower [24] explain the basic principles of hydraulic engine mounts (HEMs). HEMs having the so-called "inertia track" share the same basic principle with the designs of Goodwin [19] and Halwes [20].

Whatever kind of leverage an anti-resonant vibration isolator has, the basic operational principle is the same and all can be denoted as lever-type anti-resonant vibration isolators. All the previously mentioned systems had a single lever or equivalent, hence they only had a single anti-resonance and this limits their performance as low-pass filter-type vibration isolators. In the literature, there is not much work done in terms of using lever-type anti-resonant vibration isolators in multiple stages. One work is by Szefi [10], in which he used lever-type anti-resonant vibration isolators in connection with a mass–spring chain to achieve isolation in high-frequency ranges related to helicopter gearboxes (500 Hz–2 kHz). However, to the authors' knowledge, no study is available for low-pass filter characteristics of these systems in multiple stages.

In this paper, stop-band frequencies of various low-pass filter-type isolators will be formulated in a general framework. The aim is to show the limitations and potentials of these systems. As mentioned previously, an anti-resonant vibration isolator that utilizes DVAs will be introduced and compared with resonance-only mass–spring chains. Then, a multi-stage lever-type anti-resonant vibration isolator will be designed to achieve the lowest stop-band frequency given the overall mass of the isolator and an allowable level of transmissibility. Finally, numerical examples will be given for comparisons.

## 2. Stop-band frequency formulations

Low-pass filter-type isolators are used in applications where isolation should occur if the excitation frequency is larger than some specified frequency. The term "isolation" is quantified by the maximum allowable level of transmissibility in the isolation frequency range. Once that is given, one can calculate the stop-band frequency for any low-pass filter-type isolator and determine whether the stop-band frequency is low enough for a particular application.

In the literature, low-pass filter-type isolators that only possess resonance frequencies have been analyzed extensively. Moreover, lever-type anti-resonant vibration isolators have been analyzed to some extent. However, to the author's knowledge, there is not much work done in terms of formulating stop-band frequencies of these systems in a general framework.

In this paper, stop-band frequency formulations will be based on two non-dimensional numbers: $T_0$ and $\mu$. $T_0$ is the maximum transmissibility that is allowable in the isolation frequency range, and $\mu$ is the ratio of absorber or isolator mass to load mass. In all the calculations, the springs are assumed to be massless, linear and undamped. The masses and the base are assumed to be rigid. The base excitation motion is harmonic.

### 2.1. Resonance-only vibration isolators

#### 2.1.1. Single-degree-of-freedom mass–spring systems

The simplest and the most widely used low-pass filter-type vibration isolation system is composed of a load mass supported on a spring. The equation of motion for this system in the case of base excitation with zero damping is

$$m\ddot{x} + kx = ky, \tag{1}$$

where $y$ is the displacement of the base, $x$ is the displacement of the load, $k$ is the stiffness of the spring and $m$ is the mass of the load.

Assuming harmonic motion with frequency $\omega$:

$$x = X\mathrm{e}^{\mathrm{i}\omega t}, \quad y = Y\mathrm{e}^{\mathrm{i}\omega t}. \tag{2}$$

Transmissibility is calculated as

$$T(r) = \frac{X}{Y} = \frac{1}{1-r^2}, \quad \text{where } r = \frac{\omega}{\omega_0} \quad \text{and} \quad \omega_0 = \sqrt{\frac{k}{m}}. \tag{3}$$

In the literature transmissibility is often defined as the absolute value of the output-to-input displacement amplitude ratio. This definition enables visually appealing transmissibility versus excitation frequency graphs. However, in this paper, there will be many calculations that involve equating a transmissibility function to a particular value and solving for the frequency that satisfies that equality. To decrease the number of steps in these calculations, the transmissibility function is defined without an absolute value sign. However, for the graphs, absolute value of the transmissibility will be used.

Given a maximum allowable level of transmissibility, $T_0$, the stop-band frequency, $\omega_s$, can be calculated as

$$\frac{1}{1-\omega_s^2/\omega_0^2} = -T_0 \quad \Rightarrow \quad \omega_s = \omega_0\sqrt{1+\frac{1}{T_0}}. \tag{4}$$

Let us normalize the stop-band frequency with the natural frequency and denote it by $r_{ws}$, hence

$$r_{ws} = \omega_s/\omega_0. \tag{5}$$

Then, for this system, the normalized stop-band frequency, $r_{ws}$, is

$$r_{ws} = \frac{\omega_s}{\omega_0} = \sqrt{1+\frac{1}{T_0}}. \tag{6}$$

In all the following calculations, $r_{ws}$ will be the basis of comparisons. For every low-pass filter-type isolator design, $\omega_s$ will be calculated and it will be normalized by the natural frequency of this sdof system, which is $\omega_0$. This normalization enables that every isolation system has the same stiffness to load mass ratio. In order to distinguish $\omega_0$, $\omega_s$ and $r_{ws}$ of various systems, superscripts will be used.

### 2.1.2. *Single-degree-of-freedom mass–spring systems with inertia block*

The simplest method of decreasing $r_{ws}$ is to use an inertia block. In this method, the effective mass that the spring supports becomes the sum of the original load mass and the mass of the inertia block as depicted in Fig. 1.

For this system, the stop-band frequency can be calculated by replacing $\omega_0$ in Eq. (4) by the natural frequency of this system:

$$\omega_s^{\text{in}} = \omega_0^{\text{in}}\sqrt{1+\frac{1}{T_0}} = \sqrt{\frac{k}{m+m_{\text{is}}}}\sqrt{1+\frac{1}{T_0}}. \tag{7}$$

To calculate $r_{ws}^{\text{in}}$, let us make use of the variable $\mu$, which is the isolator mass to the load mass ratio. In this case, the isolator is considered as the spring together with the inertia block. Hence, the isolator mass is equal to the mass of the inertia block:

$$\omega_s^{\text{in}} = \sqrt{\frac{k}{m(1+\mu)}}\sqrt{1+\frac{1}{T_0}} = \omega_0\sqrt{\left(\frac{1}{1+\mu}\right)\left(1+\frac{1}{T_0}\right)}, \quad \text{where } \mu = \frac{m_{\text{is}}}{m}, \ \ \omega_0 = \sqrt{\frac{k}{m}}. \tag{8}$$

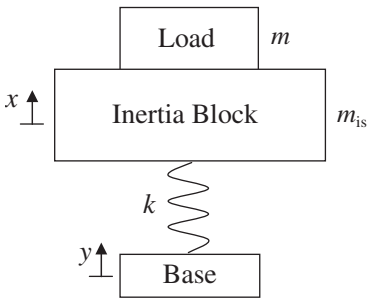


Fig. 1. Base excited sdof mass–spring system with inertia block: here, $y$ is the displacement of the base, $x$ is the displacement of the load, $k$ is the stiffness of the spring, $m$ is the mass of the load and $m_{\text{is}}$ is the mass of the inertia block.

Finally, the normalized stop-band frequency, $r_{ws}^{\text{in}}$, can be obtained as

$$r_{ws}^{\text{in}} = \frac{\omega_s^{\text{in}}}{\omega_0} = \sqrt{\left(\frac{1}{1+\mu}\right)\left(1+\frac{1}{T_0}\right)}. \tag{9}$$

When Eq. (9) is compared with Eq. (6), it can be seen that the normalized stop-band frequency decreased due to the added isolator mass.

#### 2.1.3. Multi-degree-of-freedom mass–spring chains

In this section, stop-band frequency formulas will not be derived to show the properties of these systems. However, these systems will be analyzed as a special case of another type of system, which will offer lower stop-band frequencies.

### 2.2. Anti-resonant vibration isolators

#### 2.2.1. Dynamic vibration absorber equipped springs

DVAs are generally attached to objects that are to be protected from almost constant excitation frequencies. If only vibration absorption is desired, then it is not effective to attach a DVA to the spring that supports the object (see Harris et al. [8]). On the other hand, when they are attached to springs, they can form low-pass filter-type vibration isolators, which can outperform the resonance-only isolation systems.

When passive low-pass electrical filters are investigated, it can be seen that elliptic (Cauer) filters offer the sharpest attenuation response compared to the other filters like Bessel, Butterworth or Chebyshev [5,6]. Their better performance is due to the zeros (anti-resonance frequencies) in their stop-bands. When they are converted into mechanical systems through dynamical analogies, it can be seen that the anti-resonance frequencies are generated by multiple sdof DVAs attached on a spring (see Ref. [25] for dynamical analogies). Let us analyze this DVA equipped spring as a vibration isolator. As done previously, let us denote the isolator mass to load mass ratio by $\mu$, and the isolator stiffness by $k$. The system and the variables associated with it can be seen in Fig. 2.

The equation of motion for each $m_i$ provided $1<i<n$ is

$$m_i\ddot{z}_i + k_i^a z_i = k_i^a x_i. \tag{10}$$

Moreover, $z_i$ can be obtained as a function of $x_i$'s from the force balance at the $i$th node,

$$z_i = x_i + \frac{k_{i+1}}{k_i^a}(x_i - x_{i+1}) + \frac{k_i}{k_i^a}(x_i - x_{i-1}). \tag{11}$$

Substituting Eq. (11) in Eq. (10), one can obtain

$$m_i\left(\ddot{x}_i + \frac{k_{i+1}}{k_i^a}(\ddot{x}_i - \ddot{x}_{i+1}) + \frac{k_i}{k_i^a}(\ddot{x}_i - \ddot{x}_{i-1})\right) + k_{i+1}(x_i - x_{i+1}) + k_i(x_i - x_{i-1}) = 0. \tag{12}$$

The equation of motion for $m_1$ can be obtained by replacing $x_{i-1}$ by $y$ in Eq. (12). Moreover, the equation of motion for $m_n$ is

$$m_n\ddot{x}_n + k_n x_n = k_n x_{i-1}. \tag{13}$$

The equations of motion for this system in matrix form are

$$\mathbf{MS}\ddot{\mathbf{X}} + \mathbf{KX} = \mathbf{F},$$

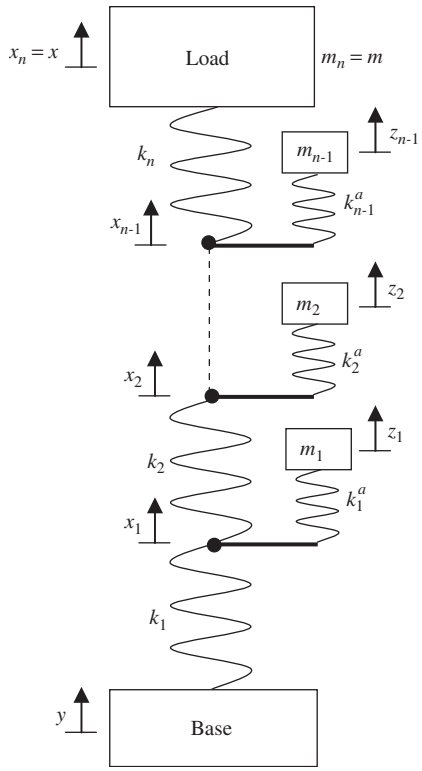


Fig. 2. Base excited $n$-dof vibration isolation system, where the isolator is an $(n-1)$-dof DVA equipped spring: here, $y$ is the displacement of the base, $x_i$ is the displacement of the $i$th stage, $k_i$ is the spring stiffness of the $i$th stage, $k_i^a$ is the spring stiffness of the $i$th absorber, and $m_i$ is the mass of the $i$th absorber except the last mass $m_n$ is the load mass. Hence, the mass of the isolator is the sum of the absorber masses.

where

$$\mathbf{M} = \begin{bmatrix} m_1 & & & \\ & m_2 & \mathbf{0} & \\ & & \ddots & \\ & \mathbf{0} & & m_n \end{bmatrix}, \quad \mathbf{X} = \begin{bmatrix} x_1 \\ x_2 \\ \vdots \\ x_n \end{bmatrix}, \quad \mathbf{F} = \begin{bmatrix} m_1 \dfrac{k_1}{k_1^a}\ddot{y} + k_1 y \\ 0 \\ \vdots \\ 0 \end{bmatrix},$$

$$\mathbf{S} = \begin{bmatrix} 1 + \dfrac{k_1 + k_2}{k_1^a} & -\dfrac{k_2}{k_1^a} & & & \\ -\dfrac{k_2}{k_2^a} & 1 + \dfrac{k_2 + k_3}{k_2^a} & -\dfrac{k_3}{k_2^a} & \mathbf{0} & \\ & \ddots & \ddots & \ddots & \\ & \mathbf{0} & -\dfrac{k_{n-1}}{k_{n-1}^a} & 1 + \dfrac{k_{n-1} + k_n}{k_{n-1}^a} & -\dfrac{k_n}{k_{n-1}^a} \\ & & & 0 & 1 \end{bmatrix},$$

$$\mathbf{K} = \begin{bmatrix} k_1 + k_2 & -k_2 & & & \\ -k_2 & k_2 + k_3 & -k_3 & & \mathbf{0} \\ & & \ddots & & \\ & & & \ddots & \\ & \mathbf{0} & & -k_{n-1} & k_{n-1} + k_n & -k_n \\ & & & & -k_n & k_n \end{bmatrix}. \tag{14}$$

Note that the mass matrix is given by the product **MS**. It can be seen that if all $k_i^a$ approach infinity, then the matrix **S** becomes an identity matrix and the system becomes an $n$-dof mass–spring chain. Now, let us assume that all $k_i^a$ are finite and compare this system with an $n$-dof mass–spring chain having the same $m_i$'s and $k_i$'s.

Assuming harmonic motion, the resonance frequencies of the system can be obtained by solving the eigenvalue problem

$$(\mathbf{MS})^{-1}\mathbf{K}\underset{\sim}{\mathrm{X}} = \omega_p^2 \underset{\sim}{\mathrm{X}}. \tag{15}$$

Besides the resonance frequencies, there are $n-1$ anti-resonance frequencies given by the resonance frequencies of the $n-1$ sdof DVAs. Hence, the $\omega_{zi}$'s are calculated as

$$\omega_{zi} = \sqrt{\frac{k_i^a}{m_i}}. \tag{16}$$

By making use of the $n$ resonance frequencies and $n-1$ anti-resonance frequencies, the transmissibility is determined as

$$T(\omega) = \frac{\prod_{i=1}^{n-1}(1 - (\omega/\omega_{zi})^2)}{\prod_{i=1}^{n}(1 - (\omega/\omega_{pi})^2)}. \tag{17}$$

The potential of the anti-resonance frequencies to lower the resonance frequencies can be fully utilized when all the anti-resonance frequencies are greater than the largest resonance frequency. Assuming both resonance and anti-resonance frequencies are indexed in increasing order, then

$$\omega_{zi} > \omega_{pn}, \quad \forall i. \tag{18}$$

Furthermore, by definition, the stop-band frequency is larger than the highest resonance frequency. Depending on the required transmissibility level, stop-band frequency can be at a frequency that is larger than some of the anti-resonance frequencies. However, a low-pass filter is most effective when the stop-band frequency is smaller than all the anti-resonance frequencies. If this is so, then the filter has better performance than an equivalent $n$-dof resonance-only filter. This will be proven in this section. However, when the stop-band frequency is, say, larger than $l$ anti-resonance frequencies, then the filter behaves similar to an $(n-l)$-dof filter. Hence, the transmissibility decay rate decreases as the stop-band frequency gets larger. Therefore, for optimum performance, let us assume that the required transmissibility level is such that

$$\omega_{pn} < \omega_s < \omega_{z1}. \tag{19}$$

Then, there is a unique $\omega_s$ solution to the equation

$$\frac{\prod_{i=1}^{n-1}(1 - (\omega_s/\omega_{zi})^2)}{\prod_{i=1}^{n}(1 - (\omega_s/\omega_{pi})^2)} = (-1)^n T_0. \tag{20}$$

Actually, in order for the solution $\omega_s$ to be qualified as a valid stop-band frequency, there is one more requirement. For all $\omega > \omega_s$, it is required that the absolute value of $T(\omega)$ be smaller than $T_0$. This requirement is always satisfied by resonance-only systems. However, for an anti-resonant system, in order for this requirement to be satisfied, $\omega_s$ needs to be smaller than $\omega_{z1}$ by a finite amount. The exact amount depends on all the poles and zeros. However, the aim in this section is to show that the stop-band frequency of this

anti-resonant system is smaller than that of an equivalent $n$-dof mass–spring chain. In order to show this, it is sufficient to know that $\omega_s < \omega_{z1}$. In order to compare the stop-band frequency of this system with an $n$-dof mass–spring chain, let us assume that $\omega_{pn} \ll \omega_s$. Therefore, the assumption is that

$$\omega_{pn} \ll \omega_s < \omega_{z1}. \tag{21}$$

Eq. (21) can be used to simplify Eq. (20) as

$$(-1)^n T_0 = \frac{\prod_{i=1}^{n-1}(1-(\omega_s/\omega_{zi})^2)}{\prod_{i=1}^{n}(1-(\omega_s/\omega_{pi})^2)} \leqslant \frac{1}{\prod_{i=1}^{n}(1-(\omega_s/\omega_{pi})^2)} \quad \text{since } 0 \leqslant \frac{\omega_s}{\omega_{zi}} < 1, \ \ \forall i. \tag{22}$$

Furthermore,

$$\frac{\omega_s}{\omega_{pi}} \gg 1 \quad \forall i \ \ \Rightarrow \ \ \frac{1}{\prod_{i=1}^{n}(1-(\omega_s/\omega_{pi})^2)} \cong \frac{1}{(-1)^n \prod_{i=1}^{n}(\omega_s/\omega_{pi})^2} = \frac{(-1)^n \prod_{i=1}^{n}\omega_{pi}^2}{\omega_s^{2n}}. \tag{23}$$

As a result,

$$(-1)^n T_0 \leqslant \frac{(-1)^n \prod_{i=1}^{n}\omega_{pi}^2}{\omega_s^{2n}} \ \ \Rightarrow \ \ \omega_s \leqslant \frac{\left(\prod_{i=1}^{n}\omega_{pi}^2\right)^{1/2n}}{(T_0)^{1/2n}}. \tag{24}$$

According to Eq. (15), $\omega_{pi}^2$ are the eigenvalues of the matrix $(\mathbf{MS})^{-1}\mathbf{K}$. For any square matrix, the product of the eigenvalues is given by the determinant. Therefore,

$$\prod_{i=1}^{n}\omega_{pi}^2 = \det((\mathbf{MS})^{-1}\mathbf{K}) = \det((\mathbf{MS})^{-1})\det(\mathbf{K}) = \frac{\det(\mathbf{K})}{\det(\mathbf{MS})} = \frac{\det(\mathbf{K})}{\det(\mathbf{M})\det(\mathbf{S})}. \tag{25}$$

Let us introduce the superscript "dva" in order to distinguish $\omega_s$ of this system from others. Moreover, let us substitute Eq. (25) in Eq. (24), then

$$\omega_s^{\mathrm{dva}} \leqslant \frac{(\det(\mathbf{K})/(\det(\mathbf{M})\det(\mathbf{S})))^{1/2n}}{(T_0)^{1/2n}}. \tag{26}$$

If the $\mathbf{S}$ matrix were an identity matrix, then the inequality in Eq. (26) would be an equality and this relation would give the stop-band frequency of the equivalent $n$-dof mass–spring chain, i.e., $\omega_s^{\mathrm{ch}}$. Therefore, the stop-band frequency of this system is indeed smaller than the stop-band frequency of the equivalent $n$-dof mass–spring chain, that is, $\omega_s^{\mathrm{dva}} < \omega_s^{\mathrm{ch}}$, provided that $\det(\mathbf{S})$ is larger than 1.

**Proposition 1.** $\det(\mathbf{S}) > 1$ *provided that* $k_i^a < \infty$ *for some* $i$.

**Proof.** According to Eq. (14), $\mathbf{S}$ is given by

$$\mathbf{S} = \begin{bmatrix} 1+\dfrac{k_1+k_2}{k_1^a} & -\dfrac{k_2}{k_1^a} & & & \\ -\dfrac{k_2}{k_2^a} & 1+\dfrac{k_2+k_3}{k_2^a} & -\dfrac{k_3}{k_2^a} & \mathbf{0} & \\ & \ddots & & & \\ & & \ddots & & \\ & \mathbf{0} & -\dfrac{k_{n-1}}{k_{n-1}^a} & 1+\dfrac{k_{n-1}+k_n}{k_{n-1}^a} & -\dfrac{k_n}{k_{n-1}^a} \\ & & & 0 & 1 \end{bmatrix}.$$

When elementary row operations are applied to a square matrix, its eigenvalues do not change. If the $\mathbf{S}$ matrix is transformed into an upper triangular matrix, then the diagonal entries are the eigenvalues. So, it is sufficient to show that all the diagonal entries of the upper triangular matrix are greater than or equal to 1, and

at least one of them is strictly greater than 1. In order to simplify the calculations, let us relabel the variables:

$$\mathbf{S}=\begin{bmatrix} 1+a_1+a_2 & -a_2 & & & & \\ -a_3 & 1+a_3+a_4 & -a_4 & & \mathbf{0} & \\ & & \ddots & & & \\ & & & \ddots & & \\ & \mathbf{0} & & -a_{2n-3} & 1+a_{2n-3}+a_{2n-2} & -a_{2n-2} \\ & & & & 0 & 1 \end{bmatrix},$$

where all $a_j \geqslant 0$, since $k_i > 0$ and $k_i^a > 0$. Moreover, $a_{2i-1}$ can be zero only when $k_i^a$ approaches infinity. Let us multiply the first row by $a_3/(1+a_1+a_2)$ and add it to the second row. Then, the matrix becomes

$$\begin{bmatrix} 1+a_1+a_2 & -a_2 & & & & \\ 0 & 1+\hat{a}_3+a_4 & -a_4 & & \mathbf{0} & \\ & -a_5 & 1+a_5+a_6 & a_7 & & \\ & & & \ddots & & \\ & \mathbf{0} & & -a_{2n-3} & 1+a_{2n-3}+a_{2n-2} & -a_{2n-2} \\ & & & & 0 & 1 \end{bmatrix},$$

where

$$\hat{a}_3 = a_3\left(\frac{1+a_1}{1+a_1+a_2}\right) \geqslant 0.$$

By successively applying this method, all the terms below the diagonal can be made equal to zero. Moreover, the diagonal terms will become $1+\hat{a}_{2i-1}+a_{2i}$, where

$$\hat{a}_{2i-1} = a_{2i-1}\left(\frac{1+\hat{a}_{2i-3}}{1+\hat{a}_{2i-3}+a_{2i-2}}\right) \geqslant 0 \quad \text{for } i = 3,4,\ldots,n-1.$$

Therefore, the first diagonal term and the others are all greater than or equal to 1. Let us relabel $a_1$ as $\hat{a}_1$, then

$$\det(\mathbf{S}) = \prod_{i=1}^{n-1}(1+\hat{a}_{2i-1}+a_{2i}).$$

If not all $k_i^a$ approach infinity, then there would be some $j$ such that $k_j^a$ is finite. Then, $a_{2j-1} > 0 \Rightarrow \hat{a}_{2j-1} > 0 \Rightarrow 1+\hat{a}_{2j-1}+a_{2j} > 1 \Rightarrow \det(\mathbf{S}) > 1$. □

Proposition 1 and Eq. (26) establishes that the stop-band frequency of this system is smaller than the stop-band frequency of an equivalent $n$-dof mass–spring chain. In other words, introduction of anti-resonance frequencies indeed improved the performance of $n$-dof vibration isolators. Now, let us illustrate the performance improvement through a numerical example.

Suppose that $n = 2$, $\mu = 0.1$. In this case, there is only one absorber on the spring and its mass is directly specified by $\mu$. Let us assume that the isolator spring stiffness values, $k_1$ and $k_2$, are equal. Hence, $k_1 = k_2 = 2k$. Let us vary the absorber spring stiffness, $k_1^a$, in order to see the effect of the anti-resonance frequency on the stop-band frequency.

If $k_1^a \to \infty$, then $\omega_z \to \infty$, and the system becomes a 2-dof mass–spring chain. Now, let us choose $k_1^a = 2.5k$, so $\omega_z = \sqrt{2.5k/0.1m} = 5\sqrt{k/m} = 5\omega_0$. Finally, let $k_1^a = 0.625k$, then $\omega_z = \sqrt{0.625k/0.1m} = 2.5\sqrt{k/m} = 2.5\omega_0$. Let us compare these three cases as three different designs, which are shown in Fig. 3.

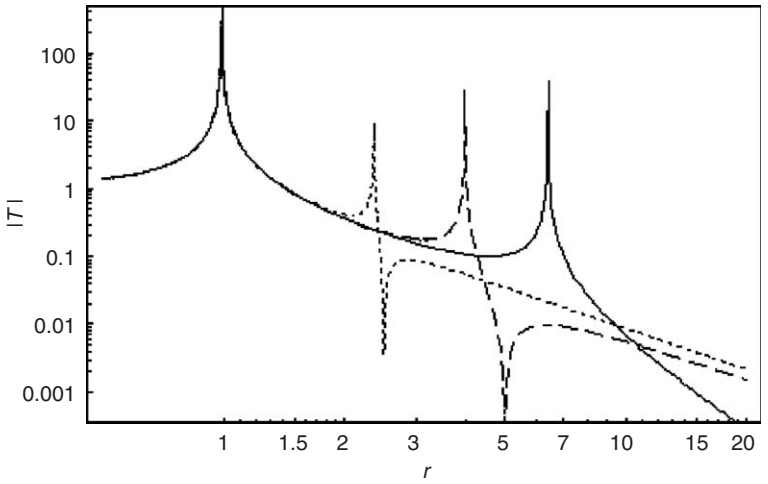


Fig. 3. Effect of anti-resonance frequency change on the stop-band frequency of a 2-dof DVA equipped spring isolation system: ———, $\omega_z/\omega_0 \to \infty$; – – – –, $\omega_z/\omega_0 = 5$; · · · · · · , $\omega_z/\omega_0 = 2.5$.

It can be seen in Fig. 3 that, as the anti-resonance frequency decreases, the higher resonance frequency of the system also decreases. If the maximum allowable transmissibility, $T_0$, is about 0.01, then the design with $\omega_z = 5\omega_0$ has the lowest stop-band frequency, $\omega_s$, among the three designs. When compared to the 2-dof mass–spring chain, $\omega_s$ of this design is about half. However, if $T_0$ is about 0.1, then the design with $\omega_z = 2.5\omega_0$ has the lowest $\omega_s$, which is approximately one-third of the 2-dof mass–spring chain value. Hence, with minimal added complexity, this system has substantially better performance than an equivalent resonance-only mass–spring chain.

In general, given $T_0$, the corresponding $\omega_z$ that minimizes $\omega_s$ is the one that makes the peak transmissibility—after the zero—equal to $T_0$. If $T_0$ gets closer to one, then $\omega_z$ can be decreased so as to minimize $\omega_s$. In that case, there would be more pronounced improvement over the 2-dof mass–spring chain. However, when $\omega_z = \sqrt{k_1^a/\mu m}$ is less than $\sqrt{k_2/m}$, then the pole-zero order changes, and the system is no longer a low-pass filter. So, there is a lower bound on $\omega_s$, which is given by $\sqrt{k_2/m}$. Since $k_2$ should always be greater than $k$, the lower bound on $\omega_s$ is larger than $\omega_0$.

As mentioned earlier, fewer degree-of-freedom isolators perform better for $T_0$ values that are not very small. The lowest degree-of-freedom DVA equipped spring isolation system is 2-dof, since there should be at least one DVA on the spring. As shown in the previous paragraph, for this system, $\omega_s$ cannot be smaller than $\omega_0$. However, if the isolator had only one pole and one zero, then $\omega_s$ could be placed at a frequency that is lower than $\omega_0$. Although this is not achievable by DVA equipped spring isolation systems, it can be attained by lever-type anti-resonant vibration isolators, which have one pole and one zero.

### 2.2.2. *Lever-type anti-resonant vibration isolators*

As mentioned in the introduction, basic operational principles of the mechanically or hydraulically leveraged anti-resonant vibration isolators are the same. For the sake of clarity in the analysis, simple levers will be used to model leverage in anti-resonant vibration isolators. Moreover, only lever-type anti-resonant vibration isolators are going to be investigated in this section. Therefore, when the term ''anti-resonant vibration isolator'' is used, it is implied that it is of ''lever-type''.

Depending on the order of the pivot points of the lever with respect to the load and the isolator mass, there are two different types of anti-resonant vibration isolators. Let us call them Type I and Type II isolators. In a Type I isolator, the pivot attached to the base is nearer to the isolator mass and in a Type II isolator, the pivot attached to the load is nearer to the isolator mass.

Let us first analyze a Type I anti-resonant vibration isolator, which is depicted in Fig. 4. Let us assume that the lever rod is massless and rigid; the spring is linear, massless and undamped. Then, the system is sdof. Moreover, let us assume that the oscillations are small. Then linear theory is applicable, generating the

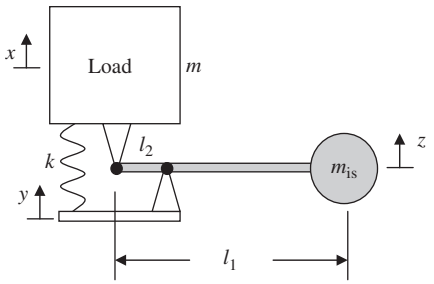


Fig. 4. Base excited Type I isolator: here, $y$ is the displacement of the base, $x$ is the displacement of the load, $z$ is the displacement of the isolator mass, $k$ is the mount stiffness, $m$ is the mass of the load, $m_{is}$ is the isolator mass, $l_1$ is the length of the lever and $l_2$ is the distance between two pivot points.

equation for $z$ in terms of $x$ and $y$ as

$$z = \alpha y - (\alpha - 1)x, \quad \text{where } \alpha = l_1/l_2 > 1. \tag{27}$$

Moreover, the equation of motion is

$$(m + m_{is}(\alpha - 1)^2)\ddot{x} + kx = (m_{is}\alpha(\alpha - 1))\ddot{y} + ky. \tag{28}$$

In order to simplify the calculations, let us use the relationships

$$\omega_0 = \sqrt{k/m}, \quad \mu = m_{is}/m. \tag{29}$$

Then, Eq. (28) can be rewritten as

$$(1 + \mu(\alpha - 1)^2)\ddot{x} + \omega_0^2 x = (\mu\alpha(\alpha - 1))\ddot{y} + \omega_0^2 y. \tag{30}$$

It is important to notice that the effective mass of the system, $(m + m_{is}(\alpha - 1)^2)$, can be much larger than $m$, provided that the lever ratio $\alpha$ is large enough. Moreover, the inertial forcing term, $m_{is}\alpha(\alpha - 1)$, also increases with the lever ratio. Thus, with a small mass $m_{is}$ one can generate large inertia forces, provided that the lever ratio is large enough.

The right-hand side of Eq. (30) can be equal to zero, when the excitation frequency is equal to

$$\omega_z = \frac{\omega_0}{\sqrt{\mu\alpha(\alpha - 1)}} = \sqrt{\frac{k}{m_{is}\alpha(\alpha - 1)}}. \tag{31}$$

Notice that $\omega_z$ is independent of $m$. Moreover, the pole of the system is at

$$\omega_p = \frac{\omega_0}{\sqrt{1 + \mu(\alpha - 1)^2}} = \sqrt{\frac{k}{m + m_{is}(\alpha - 1)^2}}. \tag{32}$$

Then, $T(\omega)$ is obtained as

$$T(\omega) = \frac{(1 - \omega^2/\omega_z^2)}{(1 - \omega^2/\omega_p^2)}. \tag{33}$$

Furthermore,

$$\frac{\omega_p}{\omega_z} = \sqrt{\frac{\mu\alpha(\alpha - 1)}{1 + \mu(\alpha - 1)^2}}. \tag{34}$$

It can be seen in Eq. (34) that if $\mu = 1/(\alpha - 1)$ then $\omega_p/\omega_z = 1$. Hence, pole and zero cancellation occurs, which imply that $T(\omega)$ is equal to one for all excitation frequencies. Moreover, given $\alpha$, if $\mu > 1/(\alpha - 1)$, then $\omega_p > \omega_z$, and if $\mu < 1/(\alpha - 1)$, then $\omega_p < \omega_z$. Therefore, the order of the pole and the zero depends upon the values of $\alpha$ and $\mu$.

In order to find the stop-band frequency, $\omega_s$, let us rewrite Eq. (33) as

$$T(\omega) = \frac{(\omega_z^2 - \omega^2)}{(\omega_p^2 - \omega^2)} \frac{\omega_p^2}{\omega_z^2}. \tag{35}$$

It can be seen that as $\omega \to \infty$, $T(\omega) \to \omega_p^2/\omega_z^2$. Assuming finite $\omega_z$ and non-zero $\omega_p$, then $T(\omega)$ converges to a positive number. Therefore, given a maximum allowable transmissibility level, $T_0$, $T(\omega)$ should converge to $T_0$ as $\omega \to \infty$. Thus, $\omega_p$ and $\omega_z$ have to satisfy the equality

$$\frac{\omega_p^2}{\omega_z^2} = T_0. \tag{36}$$

Since, $0 < T_0 < 1$, then according to Eq. (36) $\omega_p < \omega_z$, and therefore this system has the correct order of pole and zero to function as a low-pass filter-type isolator.

Finally, let us equate Eq. (35) to $-T_0$ in order to determine $\omega_s$. Let us also make use of Eq. (36), then

$$\frac{(\omega_z^2 - \omega_s^2)}{(\omega_p^2 - \omega_s^2)} T_0 = -T_0 \;\Rightarrow\; \frac{(\omega_z^2 - \omega_s^2)}{(\omega_p^2 - \omega_s^2)} = -1 \;\Rightarrow\; \omega_s = \sqrt{\frac{\omega_p^2 + \omega_z^2}{2}}. \tag{37}$$

According to Eqs. (34) and (36), $\mu$ and $\alpha$ should satisfy the equality

$$\frac{\mu\alpha(\alpha - 1)}{1 + \mu(\alpha - 1)^2} = T_0. \tag{38}$$

Eq. (38) can be used to eliminate $\alpha$ or $\mu$. To be consistent with the other $\omega_s$ calculations, $\alpha$ should be eliminated. However, the resulting equation for $\omega_s$ will not be simple to comprehend. Therefore, first $\mu$ will be eliminated and $\omega_s$ will be obtained as a function of $\omega_0$, $T_0$ and $\alpha$. After some analysis, the final form of $\omega_s$ will be given in terms of $\omega_0$, $T_0$ and $\mu$.

Let us use Eq. (36) in Eq. (37) to eliminate $\omega_z$ and further use Eq. (32) to obtain the relation

$$\omega_s = \sqrt{\frac{\omega_p^2}{2}\left(1 + \frac{1}{T_0}\right)} = \frac{\omega_0}{\sqrt{2}} \sqrt{\frac{1}{1 + \mu(\alpha - 1)^2}\left(1 + \frac{1}{T_0}\right)}. \tag{39}$$

Consequently, let us solve for $\mu$ in Eq. (38):

$$\mu = \frac{T_0}{\alpha(\alpha - 1) - T_0(\alpha - 1)^2}. \tag{40}$$

By substituting Eq. (40) in Eq. (39), $\omega_s$ can be obtained as a function of $\omega_0$, $T_0$ and $\alpha$. Furthermore, let us introduce the superscript "$I$" in order to distinguish $\omega_s$ of this system from others. Then,

$$\omega_s^I = \frac{\omega_0}{\sqrt{2}} \sqrt{\left(1 - T_0\left(1 - \frac{1}{\alpha}\right)\right)\left(1 + \frac{1}{T_0}\right)} = \frac{\omega_0}{\sqrt{2}} \sqrt{\frac{1 + T_0}{\alpha} + \frac{1}{T_0} - T_0}. \tag{41}$$

Let us finally calculate $r_{ws}^I$, using the definition given by Eq. (5):

$$r_{ws}^I = \frac{\omega_s^I}{\omega_0} = \sqrt{\frac{1}{2}\left(1 - T_0\left(1 - \frac{1}{\alpha}\right)\right)\left(1 + \frac{1}{T_0}\right)} = \sqrt{\frac{1}{2}\left(\frac{1 + T_0}{\alpha} + \frac{1}{T_0} - T_0\right)}. \tag{42}$$

Since this is a sdof system, let us compare Eq. (42) with Eq. (6) or Eq. (9). By definition, the lever ratio, $\alpha$, should be greater than one. The upper limit on $\alpha$ is dictated by physical limitations. Suppose that there is no upper limit or it is very large. Then,

$$\alpha \to \infty \;\Rightarrow\; r_{ws}^I \to \sqrt{\frac{1}{2}\left(\frac{1}{T_0} - T_0\right)}. \tag{43}$$

According to Eq. (40), given $T_0$, as $\alpha \to \infty$ then $\mu \to 0$. So, let us compare this case with Eq. (6) since it is derived for a massless sdof isolator:

$$\alpha \to \infty \;\Rightarrow\; r_{ws}^I \to \sqrt{\frac{1}{2}\left(\frac{1}{T_0} - T_0\right)} < \sqrt{\left(\frac{1}{T_0} - T_0\right)} < \sqrt{\left(\frac{1}{T_0} + 1\right)} = r_{ws} \;\Rightarrow\; r_{ws}^I < \frac{r_{ws}}{\sqrt{2}}. \tag{44}$$

Therefore, as $\alpha \to \infty$, the Type I isolator performs better than an equivalent sdof mass–spring system. Moreover, $r_{ws}^I$ can be considerably smaller than the upper bound given in Eq. (44) if the transmissibility requirement, $T_0$, is not very small. In fact, according to Eq. (43), $r_{ws}^I$ is smaller than one, if $T_0 > \sqrt{2} - 1 \cong 0.41$. In other words, if $T_0 > 0.41$, then $\omega_s^I$ is smaller than $\omega_0$. As shown at the end of Section 2.2.1, this is not achievable by DVA equipped spring isolation systems.

It can be seen from Eq. (42) that given $T_0$, if $\alpha$ gets smaller, then $r_{ws}^I$ gets larger. In other words, as $\mu$ increases, the performance of a Type I isolator decreases. This behavior is opposite to sdof mass–spring systems with inertia block. According to Eq. (9), as $\mu$ increases the performance increases, i.e., $r_{ws}^{\text{in}}$ gets smaller.

Let us finally obtain $\omega_s^I$ as a function of $\omega_0$, $T_0$ and $\mu$. To do that, let us solve for $\alpha$ in Eq. (38). Let us use the property that $\alpha$ should be greater than one, then

$$\alpha = \frac{(1 - 2T_0) + \sqrt{1 + (4T_0/\mu) - (4T_0^2/\mu)}}{2(1 - T_0)}. \tag{45}$$

Now, let us use Eq. (45) in Eq. (41):

$$\omega_s^I = \omega_0 \sqrt{\left(\frac{(1 - T_0)^2}{2 + \mu - 2T_0 - \sqrt{\mu^2 + 4\mu T_0 - 4\mu T_0^2}}\right)\left(1 + \frac{1}{T_0}\right)}. \tag{46}$$

Therefore, $r_{ws}^I$ as a function of $T_0$ and $\mu$ is

$$r_{ws}^I = \sqrt{\left(\frac{(1 - T_0)^2}{2 + \mu - 2T_0 - \sqrt{\mu^2 + 4\mu T_0 - 4\mu T_0^2}}\right)\left(1 + \frac{1}{T_0}\right)}. \tag{47}$$

As an example, let $T_0 = 0.1$ and $\mu = 0.1$. Fig. 5 shows the transmissibility plots of a Type I isolator and a sdof mass–spring system with inertia block.

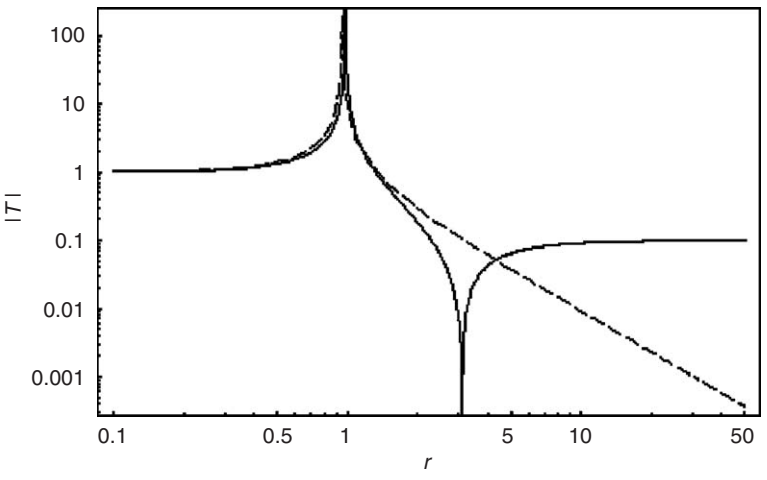


Fig. 5. Transmissibility plots showing the stop-band frequencies of a Type I isolator (———) and a sdof mass–spring system with inertia block (– – – –) for $T_0 = 0.1$ and $\mu = 0.1$.

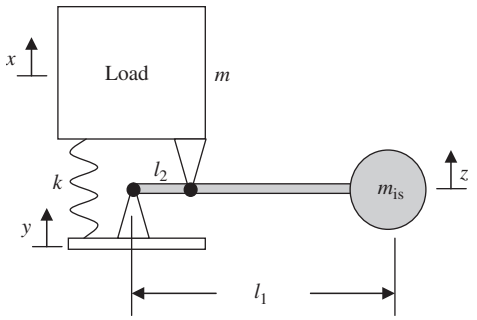


Fig. 6. Base excited Type II isolator: here, $y$ is the displacement of the base, $x$ is the displacement of the load, $z$ is the displacement of the isolator mass, $k$ is the mount stiffness, $m$ is the mass of the load, $m_{is}$ is the isolator mass, $l_1$ is the length of the lever and $l_2$ is the distance between two pivot points.

According to Eq. (47), $r_{ws}^{I}$ can be calculated as 2.30. Moreover, using Eq. (9), $r_{ws}^{in}$ can be calculated as 3.16. Hence, there is 27% of improvement.

Now, let us formulate the stop-band frequency of a Type II anti-resonant vibration isolator, which is shown in Fig. 6.

The equation of motion is

$$(1+\mu\alpha^2)\ddot{x}+\omega_0^2 x=(\mu\alpha(\alpha-1))\ddot{y}+\omega_0^2 y, \quad \text{where } \omega_0=\sqrt{k/m}, \quad \mu=m_{is}/m, \quad \alpha=l_1/l_2. \tag{48}$$

In a Type II isolator, the effective mass of the system is larger. Hence, the pole of a Type II isolator is smaller than that of an equivalent Type I isolator:

$$\omega_p=\frac{\omega_0}{\sqrt{1+\mu\alpha^2}}=\sqrt{\frac{k}{m+m_{is}\alpha^2}}. \tag{49}$$

$\omega_z$ is the same with an equivalent Type I isolator, which is given in Eq. (31). Moreover,

$$\frac{\omega_p}{\omega_z}=\sqrt{\frac{\mu\alpha(\alpha-1)}{1+\mu\alpha^2}}<1 \quad \text{for } \alpha>1. \tag{50}$$

By definition, $\alpha$ is greater than one. Hence, in a Type II isolator $\omega_p$ is always less than $\omega_z$. It can be seen that by replacing $\alpha$ with $(1-\alpha)$ in Eq. (48) one can obtain Eq. (30). Hence, the stop-band frequency of a Type II isolator can be obtained by replacing $\alpha$ with $(1-\alpha)$ in Eq. (41). Then,

$$\omega_s^{II}=\frac{\omega_0}{\sqrt{2}}\sqrt{\left(1-T_0\left(\frac{\alpha}{\alpha-1}\right)\right)\left(1+\frac{1}{T_0}\right)}=\frac{\omega_0}{\sqrt{2}}\sqrt{\frac{1+T_0}{1-\alpha}+\frac{1}{T_0}-T_0}. \tag{51}$$

So, $r_{ws}^{II}$ can be calculated as

$$r_{ws}^{II}=\frac{\omega_s^{II}}{\omega_0}=\sqrt{\frac{1}{2}\left(1-T_0\left(\frac{\alpha}{\alpha-1}\right)\right)\left(1+\frac{1}{T_0}\right)}=\sqrt{\frac{1}{2}\left(\frac{1+T_0}{1-\alpha}+\frac{1}{T_0}-T_0\right)}. \tag{52}$$

It can be seen that as $\alpha\to\infty$, $r_{ws}^{II}$ converges to the same equation as $r_{ws}^{I}$ does in Eq. (43). So, in this case, the Type II isolator has the same properties of an equivalent Type I isolator. However, according to Eq. (52), given $T_0$, if $\alpha$ gets smaller then $r_{ws}^{II}$ also gets smaller. In other words, as $\mu$ increases the performance of a Type II isolator does not decrease as in the case of a Type I isolator, but the performance also increases.

Now, let us obtain $\omega_s^{II}$ as a function of $\omega_0$, $T_0$ and $\mu$. To do that let us equate $\omega_p^2/\omega_z^2$ to $T_0$ in Eq. (50) and solve for $\alpha$ as a function of $T_0$ and $\mu$. Hence,

$$\alpha=\frac{1+\sqrt{1+(4T_0/\mu)-(4T_0^2/\mu)}}{2(1-T_0)}. \tag{53}$$

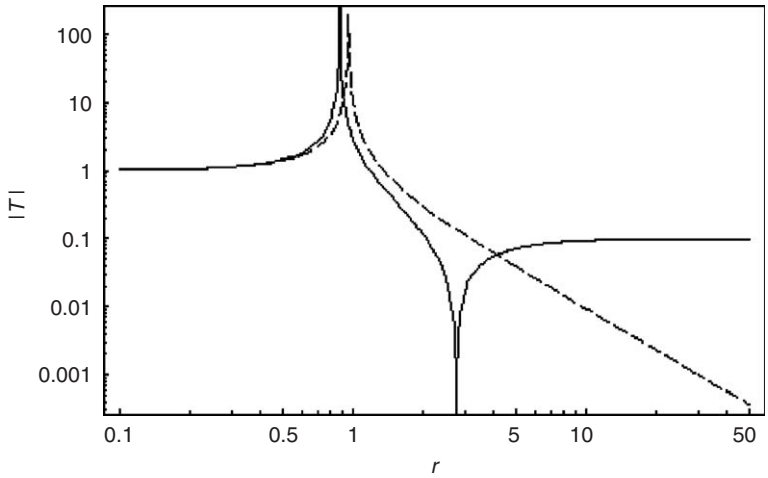


Fig. 7. Transmissibility plots showing the stop-band frequencies of a Type II isolator (———) and a sdof mass–spring system with inertia block (– – – –) for $T_0 = 0.1$ and $\mu = 0.1$.

Then, let us substitute Eq. (53) in Eq. (51):

$$\omega_s^{II} = \omega_0 \sqrt{\left(\frac{(1-T_0)^2}{2+\mu-2T_0+\sqrt{\mu^2+4\mu T_0-4\mu T_0^2}}\right)\left(1+\frac{1}{T_0}\right)}. \tag{54}$$

Finally, $r_{ws}^{II}$ as a function of $T_0$ and $\mu$ can be obtained as

$$r_{ws}^{II} = \sqrt{\left(\frac{(1-T_0)^2}{2+\mu-2T_0+\sqrt{\mu^2+4\mu T_0-4\mu T_0^2}}\right)\left(1+\frac{1}{T_0}\right)}. \tag{55}$$

Let us now compare a Type II isolator with an equivalent sdof mass–spring system with inertia block. As an example, let $T_0 = 0.1$ and $\mu = 0.1$. Fig. 7 shows the transmissibility plots of a Type II isolator and a sdof mass–spring system with inertia block.

According to Eq. (55), $r_{ws}^{II}$ can be calculated as 2.05. Moreover, using Eq. (9), $r_{ws}^{\text{in}}$ can be calculated as 3.16. Hence, there is 35% of improvement.

### 2.3. Stop-band frequency comparisons

As discussed before, few degree-of-freedom isolation systems perform better at transmissibility levels that are not very small. The lowest degree-of-freedom isolators having non-zero isolator mass are: sdof mass–spring systems with inertia block, 2-dof DVA equipped spring isolation systems and finally, Type I and Type II anti-resonant vibration isolators. It has been shown that 2-dof DVA equipped spring isolation systems cannot have $\omega_s$ smaller than $\omega_0$. Equivalently, $r_{ws}$ for these systems is always larger than one. However, according to Eqs. (42) and (52), $r_{ws}^{I}$ and $r_{ws}^{II}$ can be less than one. Moreover, according to Eq. (9), $r_{ws}^{\text{in}}$ can also be less than one. The aim in this section is to compare the systems that can have $r_{ws}$ smaller than one. Based on these comparisons, higher degree-of-freedom systems will be synthesized in the next section.

In order to compare $r_{ws}^{\text{in}}$, $r_{ws}^{I}$ and $r_{ws}^{II}$, all of them should be given in terms of the same variables. Thus, let us compare Eqs. (9), (47) and (55):

$$r_{ws}^{I}=\sqrt{\left(\frac{(1-T_0)^2}{2+\mu-2T_0-\sqrt{\mu^2+4\mu T_0-4\mu T_0^2}}\right)\left(1+\frac{1}{T_0}\right)},\quad r_{ws}^{\text{in}}=\sqrt{\left(\frac{1}{1+\mu}\right)\left(1+\frac{1}{T_0}\right)},$$

$$r_{ws}^{II}=\sqrt{\left(\frac{(1-T_0)^2}{2+\mu-2T_0+\sqrt{\mu^2+4\mu T_0-4\mu T_0^2}}\right)\left(1+\frac{1}{T_0}\right)}.$$

First of all, it is clear that $r_{ws}^{II}$ is always smaller than $r_{ws}^{I}$. These relationships only differ by a sign in front of the square-root term in the denominator. By definition, $\mu > 0$ and $0<T_0<1$. So, the term $2+\mu-2T_0$ is positive. Moreover, $(1-T_0)^2$ is also positive. Hence, the positive sign in front of the square-root term implies that $r_{ws}^{II}$ is always smaller than $r_{ws}^{I}$.

Now, let us show that $r_{ws}^{II}$ is always smaller than $r_{ws}^{\text{in}}$. In order to do that, it is enough to show that the following inequality is satisfied for all $\mu>0$ and $0<T_0<1$:

$$\left(\frac{(1-T_0)^2}{2+\mu-2T_0+\sqrt{\mu^2+4\mu T_0-4\mu T_0^2}}\right)<\left(\frac{1}{1+\mu}\right). \tag{56}$$

However,

$$\begin{aligned}\mu>0,\ \ 0<T_0<1 &\Rightarrow \sqrt{\mu^2+4\mu T_0-4\mu T_0^2}>\mu\\ &\Rightarrow \left(\frac{(1-T_0)^2}{2+\mu-2T_0+\sqrt{\mu^2+4\mu T_0-4\mu T_0^2}}\right)<\left(\frac{(1-T_0)^2}{2+2\mu-2T_0}\right).\end{aligned} \tag{57}$$

According to Eqs. (56) and (57) it is enough to show that

$$\begin{aligned}\frac{(1-T_0)^2}{2(1+\mu-T_0)}<\frac{1}{1+\mu} &\Leftrightarrow (1-T_0)^2(1+\mu)<2(1+\mu-T_0)\\ &\Leftrightarrow(-1-2T_0+T_0^2)(1+\mu)+2T_0<0\Leftrightarrow(\mu)(-1-2T_0+T_0^2)\\ &\quad+(-1+T_0^2)<0.\end{aligned} \tag{58}$$

Moreover,

$$\begin{aligned}0<T_0<1 &\Rightarrow (-1+T_0^2)<0,\ \ (-1-2T_0+T_0^2)<0.\\ \mu>0 &\Rightarrow (\mu)(-1-2T_0+T_0^2)<0.\end{aligned} \tag{59}$$

Therefore,

$$(\mu)(-1-2T_0+T_0^2)+(-1+T_0^2)<0. \qquad \square$$

It has been shown that the Type II isolator has the best performance among the previously mentioned designs. Let us now illustrate the performance of these systems graphically. Fig. 8 shows the dependence of $r_{ws}$ to $\mu$, given $T_0=0.1$ and Fig. 9 demonstrates the dependence of $r_{ws}$ to $T_0$, given $\mu=0.1$.

It can be seen from Fig. 8 that Type II isolator has the lowest $r_{ws}$ for all $\mu$ values. As mentioned in Section 2.3.2, $r_{ws}^{I}$ is lowest when $\mu=0$. Furthermore, it can be seen that in order to obtain an $r_{ws}$ value of 1, one needs an inertia block having a mass of $10m$, where $m$ is the mass of the load. However, by using a Type II isolator, the same $r_{ws}$ value can be achieved if the isolator mass is approximately $3.5m$.

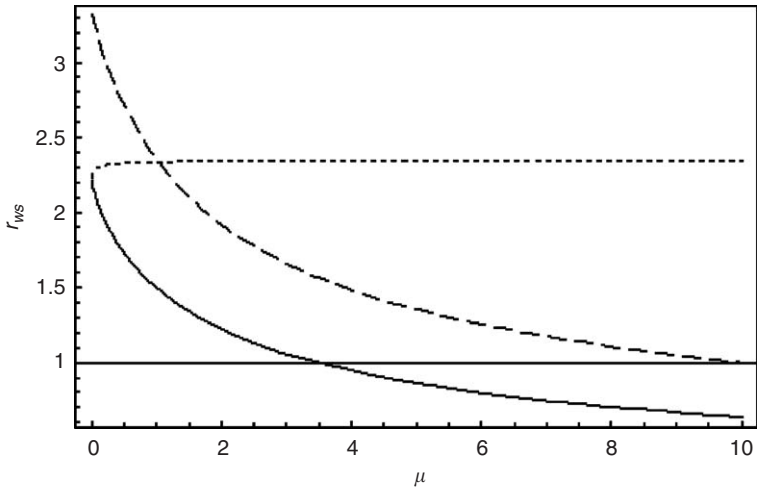


Fig. 8. $r_{ws}$ versus $\mu$ comparisons for sdof mass–spring system with inertia block (– – – –), Type I isolator (· · · · · ·) and Type II isolator (———) given $T_0 = 0.1$.

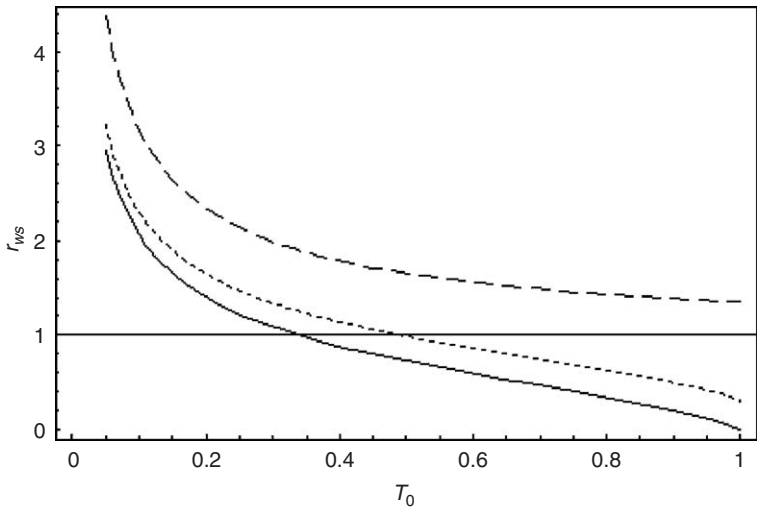


Fig. 9. $r_{ws}$ versus $T_0$ comparisons for sdof mass–spring system with inertia block (– – – –), Type I isolator (· · · · · ·) and Type II isolator (———) given $\mu = 0.1$.

It can be seen from Fig. 9 that the Type II isolator has the lowest $r_{ws}$ for all $T_0$ values. Moreover, it can be observed that the sdof mass–spring system with inertia block cannot reach $r_{ws} = 1$. However, the Type I isolator reaches $r_{ws} = 1$ at about $T_0 = 0.5$ and the Type II isolator reaches it at about $T_0 = 0.35$.

## 3. Design of stiff low-pass filter-type vibration isolators

In Section 2, stop-band frequencies of low-pass filter-type isolators were derived assuming that they all have the same overall stiffness to load mass ratio. Equivalently, the overall stiffness of all the designs can be chosen such that every design has the same stop-band frequency for a given level of transmissibility. So, the designs that have the smallest stop-band frequencies in the first case would be the stiffest in the second case.

The aim in this section is to obtain vibration isolators that can outperform the existing designs at low transmissibility levels. This can be achieved through mdof low-pass filter-type vibration isolators that have an equal number of poles and zeros.

### 3.1. Building blocks

In Section 2.3, it has been proven that among the lowest degree-of-freedom isolator designs, Type II anti-resonant vibration isolators yielded the lowest stop-band frequency for any $\mu>0$ and $0<T_0<1$. Moreover, these designs can be combined in series to obtain mdof systems having an equal number of poles and zeros. One major requirement is that these mdof systems should have the correct order of poles and zeros, that is, all the poles should precede all the zeros.

According to Eq. (50), Type II isolators always have the correct pole-zero order. However, when they are combined in series, the order of poles and zeros may shuffle. Hence, certain constraints should be imposed in order to obtain the correct pole-zero order, which will be discussed later.

Now, let us analyze the $n$-dof isolator composed of Type II isolators as shown in Fig. 10. In short, let us denote this system as an $n$-dof Type II isolator.

The equation of motion for the $i$th stage is, provided that $1<i<n$,

$$\begin{bmatrix} -m_i\alpha_i(\alpha_i-1) & m_i^S+m_{i+1}(\alpha_{i+1}-1)^2+m_i(\alpha_i)^2 & -m_{i+1}\alpha_{i+1}(\alpha_{i+1}-1) \end{bmatrix} \begin{bmatrix} \ddot{x}_{i-1} \\ \ddot{x}_i \\ \ddot{x}_{i+1} \end{bmatrix} + \begin{bmatrix} -k_i & k_i+k_{i+1} & -k_{i+1} \end{bmatrix} \begin{bmatrix} x_{i-1} \\ x_i \\ x_{i+1} \end{bmatrix} = 0. \tag{60}$$

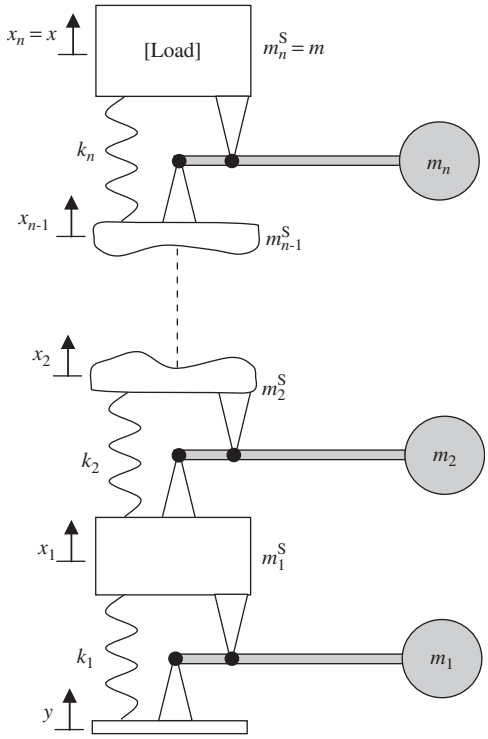


Fig. 10. Base excited $n$-dof Type II isolator: here, $y$ is the displacement of the base, $x_i$ is the displacement of the $i$th stage, $m_i^S$ is the mass of the $i$th stage, $m_i$ is the mass of the $i$th isolator, $\alpha_i$ is the lever ratio of the $i$th isolator, and $k_i$ is the spring stiffness of the $i$th stage. It can be seen that load is in the uppermost stage.

The equation of motion for the first stage can be obtained by replacing $x_{i-1}$ by $y$ in Eq. (60). Moreover, the equation of motion for the last stage is

$$[-m_n\alpha_n(\alpha_n-1) \quad m_n^S+m_n(\alpha_n)^2]\begin{bmatrix}\ddot{x}_{n-1}\\ \ddot{x}_n\end{bmatrix}+[-k_n \quad k_n]\begin{bmatrix}x_{n-1}\\ x_n\end{bmatrix}=0. \tag{61}$$

The equations of motion for this system in matrix form are

$$\mathbf{M}\ddot{\mathbf{X}}+\mathbf{K}\mathbf{X}=\mathbf{F}, \tag{62}$$

where

$$\mathbf{M}=\begin{bmatrix} m_1^S+m_1(\alpha_1)^2+m_2(\alpha_2-1)^2 & -m_2\alpha_2(\alpha_2-1) & & & \\ -m_2\alpha_2(\alpha_2-1) & m_2^S+m_2(\alpha_2)^2+m_3(\alpha_3-1)^2 & -m_3\alpha_3(\alpha_3-1) & \mathbf{0} & \\ & \cdot & & & \\ & & \cdot & & \\ & \mathbf{0} & & \cdot & \\ & & & -m_n\alpha_n(\alpha_n-1) & m_n^S+m_n(\alpha_n)^2 \end{bmatrix},$$

$$\mathbf{K}=\begin{bmatrix} k_1+k_2 & -k_2 & & & \\ -k_2 & k_2+k_3 & -k_3 & \mathbf{0} & \\ & \cdot & & & \\ & & \cdot & & \\ \mathbf{0} & & -k_{n-1} & k_{n-1}+k_n & -k_n \\ & & & -k_n & k_n \end{bmatrix}, \quad \mathbf{X}=\begin{bmatrix}x_1\\ x_2\\ \cdot\\ \cdot\\ \cdot\\ x_n\end{bmatrix},$$

$$\mathbf{F}=\begin{bmatrix}k_1 y+m_1\alpha_1(\alpha_1-1)\ddot{y}\\ 0\\ \cdot\\ \cdot\\ \cdot\\ 0\end{bmatrix}.$$

Assuming harmonic motion, the resonance frequencies of the system can be obtained by solving the eigenvalue problem

$$\mathbf{M}^{-1}\mathbf{K}\underset{\sim}{\mathrm{X}}=\omega_p^2\underset{\sim}{\mathrm{X}}. \tag{63}$$

Besides the $n$ resonance frequencies, there are $n$ anti-resonance frequencies in this system. $n-1$ of the anti-resonance frequencies are obtained by equating the off-diagonal terms of the matrix $\mathbf{K}-\omega_z^2\mathbf{M}$ to zero, and the last one comes from equating the forcing term to zero. They are all in the form

$$\omega_{zi}=\sqrt{\frac{k_i}{m_i\alpha_i(\alpha_i-1)}}. \tag{64}$$

By making use of the $n$ resonance frequencies and $n$ anti-resonance frequencies, transmissibility is determined as

$$T(\omega)=\frac{\prod_{i=1}^{n}(1-(\omega/\omega_{zi})^2)}{\prod_{i=1}^{n}(1-(\omega/\omega_{pi})^2)}. \tag{65}$$

In order for this system to function as a low-pass filter, all the zeros should be after the highest pole. Assuming both poles and zeros are indexed in increasing order, then

$$\omega_{pn} < \omega_{z1}. \tag{66}$$

Subsequently, once all the poles and zeros are known and $T_0$ is given, the stop-band frequency, $\omega_s$, can be determined uniquely from the equality

$$\frac{\prod_{i=1}^{n}(1-(\omega_s/\omega_{zi})^2)}{\prod_{i=1}^{n}(1-(\omega_s/\omega_{pi})^2)} = (-1)^n T_0. \tag{67}$$

### 3.2. The optimization problem

In a sdof Type II isolator, mount stiffness $k$ and the load mass $m$ are the parameters that are used to scale the resonance and anti-resonance frequencies of the system. Once the constraints $T_0$ and $\mu$ are known, the two variables that define the system, $\alpha$ and $m_{\text{is}}$, are determined uniquely. However, in an $n$-dof Type II isolator there are more variables than the number of constraints. As a result, there is the opportunity of minimizing the stop-band frequency through optimization.

Before stating the optimization problem, let us make some explanations. In this system, the aim is to group the $n$ zeros after the highest pole. In that case, there will be $(n-1)$ local peaks in the transmissibility function until the function converges to a constant value. Let us index the peaks in increasing order and let $\omega^i_{\text{peak}}$ be the $i$th peak frequency. The statement of the optimization problem is as follows:

$$\begin{aligned}
&\text{minimize} && \omega_s \\
&\text{subject to} && \mathrm{h}_i : T(\omega^i_{\text{peak}}) = (-1)^{n+i} T_0 \ \text{ for } i = 1, 2, \ldots, n-1, \\
&&& \mathrm{h}_n : T(\infty) = T_0, \\
&&& \mathrm{h}_{n+1} : \sum_{i=1}^{n-1} m_i^S + \sum_{i=1}^{n} m_i = \mu m, \\
&&& \mathrm{h}_{n+2} : \sum_{i=1}^{n} \frac{1}{k_i} = \frac{1}{k}, \\
&&& \mathrm{g}_1 : \omega_{pn} < \omega_{z1}, \\
&&& k_i \geqslant k, \ \ m_i \geqslant 0, \ \ \alpha_i \geqslant 1, \ \ \text{for } i = 1, 2, \ldots, n, \\
&&& m_i^S \geqslant 0 \ \ \text{for } i = 1, 2, \ldots, n-1.
\end{aligned}$$

There are $(4n-1)$ variables and $(n+2)$ equality constraints in this problem. Therefore, the solution space is $(3n-3)$ dimensional. As mentioned earlier, for the case of $n=1$, there is a unique solution. However, if $n>1$, then there is room for optimization.

In order to obtain some quantitative results, let us try to solve the optimization problem for the case of $n=2$. There are seven variables in this problem, which are $m_1$, $m_2$, $\alpha_1$, $\alpha_2$, $k_1$, $k_2$ and $m_1^S$.

Let us focus on the variable $m_1^S$. This variable represents the mass of the first stage and it will be shown that in order to achieve low pole values, or equivalently low stop-band frequency, this variable should be equated to zero.

Similar to Eq. (25), the product of the poles of this system is given by $\det(\mathbf{K})/\det(\mathbf{M})$. Hence, in order to lower the values of the poles, $\det(\mathbf{K})/\det(\mathbf{M})$ should be decreased. Since $\mathbf{K}$ is independent of the variable $m_1^S$, let us just consider $\det(\mathbf{M})$. According to Eq. (61), $\det(\mathbf{M})$ can be calculated as

$$\det(\mathbf{M}) = (m_1^S + m_1(\alpha_1)^2 + m_2(\alpha_2-1)^2)(m + m_2(\alpha_2)^2) - (m_2\alpha_2(\alpha_2-1))^2. \tag{68}$$

Given $m$ and $\mu$, there is a constraint on the sum of the values of $m_1$, $m_2$ and $m_1^S$ as stated in the optimization problem. If $\alpha_1 > 1$, then $m_1(\alpha_1)^2 > m_1^S$ provided $m_1 = m_1^S$. So, if the sum of $m_1$ and $m_1^S$ is given then $m_1(\alpha_1)^2 + m_1^S$ is maximum when $m_1^S = 0$. However, in order to have a lever, $\alpha_1$ should be greater than one. Therefore, to maximize the value of $\det(\mathbf{M})$, $m_1^S$ should be equal to zero. Through mathematical induction, one can show that the above argument is also valid for $n$-dof systems, i.e., $m_i^S$ should be equal to zero for $i = 1, 2, \ldots, n-1$.

This then reduces the number of variables in an $n$-dof system to $3n$. Therefore, the solution space of the problem becomes $(2n-2)$ dimensional.

Let us again concentrate on the problem when $n=2$. After elimination of the variable $m_1^S$, the number of variables in the optimization problem reduces to 6, which are $k_1$, $k_2$, $m_1$, $m_2$, $\alpha_1$ and $\alpha_2$. There are six variables and four equality constraints. Let us call the variables $k_2$, $m_2$, $\alpha_1$ and $\alpha_2$ as state variables that satisfy the four equality constraints. The remaining two variables, $k_1$ and $m_1$, are called the decision variables.

The state variables $m_2$ and $k_2$ can easily be solved in terms of the decision variables using equality constraints $h_3$ and $h_4$, respectively. Although, $\omega_s$, $\omega^1_{\text{peak}}$ and $T(\omega^1_{\text{peak}})$ can be determined analytically, it is not feasible to solve for $\alpha_1$ and $\alpha_2$ analytically using the equality constraints $h_1$ and $h_2$. However, $\alpha_1$ and $\alpha_2$ can easily be determined via Newton's method using the equality constraints $h_1$ and $h_2$. To determine the values of the decision variables that minimize $\omega_s$, any gradient-based algorithm can be used. In this paper, Newton's method with variable step length is used in order not to violate the set constraints and the inequality constraint $g_1$.

For some $\mu$ and $T_0$ values the optimum appeared at the boundary of the solution space and for others the optimum was in the interior. Given $\mu$ and $T_0$, to check whether the local minimum obtained through the optimization routine is actually a global minimum, different initial conditions are used. It has been observed that all the initial conditions gave the same outputs whether it is a boundary or an interior solution. Therefore, it is highly probable that the search space has a single minimum for any reasonable value of $\mu$ and $T_0$.

### 3.3. Numerical results

Let us compare the designs obtained through the optimization routine with the equivalent Type II isolators, which after all offer the smallest stop-band frequency among the lowest degree-of-freedom isolation systems. In all the comparisons, let $k=1$ and $m=1$.

Let us first choose $\mu=0.1$ and $T_0=0.1$. For the Type II isolator, $\mu=0.1$, $m=1 \Rightarrow m_{\text{is}}=0.1$. Moreover, $\mu=0.1$, $T_0=0.1 \Rightarrow \alpha=1.747$. For the 2-dof optimum design, the values of the variables are: $m_1=0.09818$, $m_2=0.00182$, $k_1=9.836$, $k_2=1.113$, $\alpha_1=6.172$, $\alpha_2=9.370$. Fig. 11 shows the transmissibility plots of the two systems.

By using Eq. (55), normalized stop-band frequency of the Type II isolator, $r^{II}_{ws}$, can be found as 2.05. Moreover, the normalized stop-band frequency of the 2-dof optimum design, $r^{\text{op}}_{ws}$, is calculated as 1.75. Let $R_{rws}$ be the ratio of $r^{\text{op}}_{ws}$ to $r^{II}_{ws}$. Then, $R_{rws}=0.852$. Hence, the stop-band frequency of the optimum design is 85% of the Type II isolator's.

It can be seen that although $R_{rws}$ is less than one, the pole and zero values are quite close in the optimum design. This is not a desirable property, since isolation characteristics deteriorate quite abruptly near the

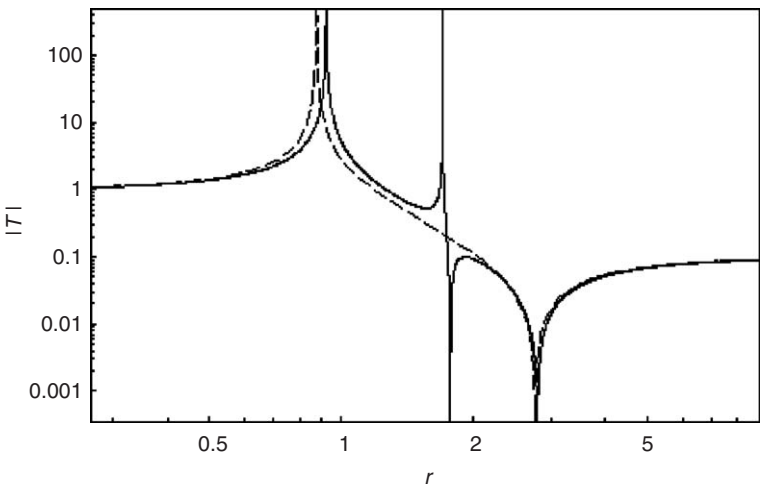


Fig. 11. Stop-band frequency comparison of a Type II isolator (– – – –) and the 2-dof optimum design (———) for $\mu=0.1$ and $T_0=0.1$.

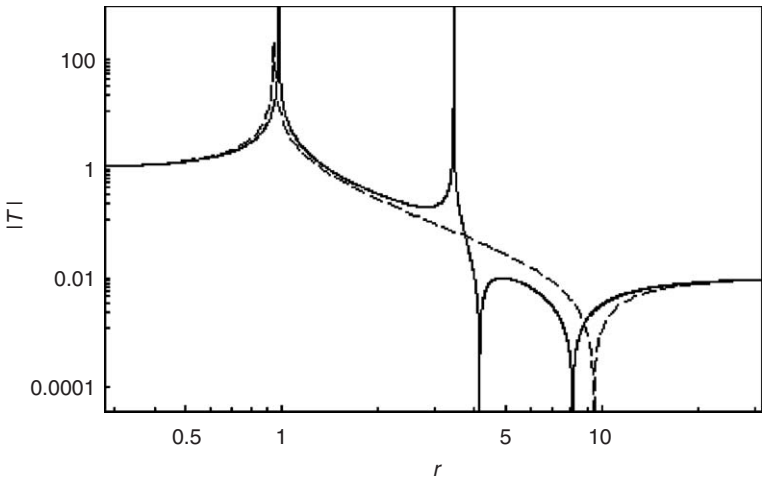


Fig. 12. Stop-band frequency comparison of a Type II isolator (– – – –) and the 2-dof optimum design (———) for $\mu = 0.1$ and $T_0 = 0.01$.

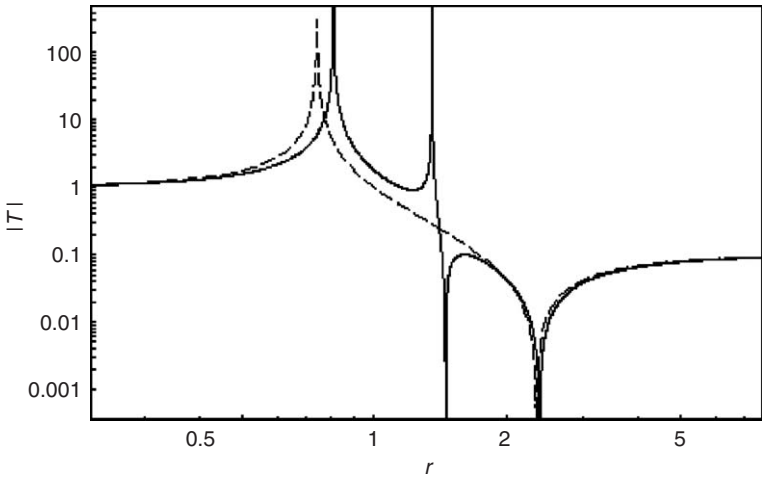


Fig. 13. Stop-band frequency comparison of a Type II isolator (– – – –) and the 2-dof optimum design (———) for $\mu = 0.5$ and $T_0 = 0.1$.

stop-band frequency. However, if a lower level of transmissibility were required, then the pole-zero separation would be larger. To see this numerically, let us keep $\mu = 0.1$ and decrease $T_0$ to 0.01. Then, for the Type II isolator, $m_{is} = 0.1$ and $\alpha = 1.102$. However, for the 2-dof design, the optimum is achieved when $m_2 \to 0$. In that case, $\alpha_2 \to \infty$. However, this is physically not realizable. Besides, $k_1$ converges to a number close to 3.80. Nevertheless, the value of $r_{ws}$ changes negligibly if $\alpha_2 > 14$. So, let us choose $m_1$ as 0.0999 and $k_1$ as 3.80 and obtain the rest of the variables using the constraint equations. Here are the values of the variables for the 2-dof quasi-optimal design: $m_1 = 0.0999$, $m_2 = 0.0001$, $k_1 = 3.8$, $k_2 = 1.357$, $\alpha_1 = 2.066$, $\alpha_2 = 14.89$. Fig. 12 shows the transmissibility plots of the two systems.

In this case, the normalized stop-band frequency of the Type II isolator can be found to be 6.71. Moreover, the normalized stop-band frequency of the 2-dof quasi-optimal design is calculated as 4.00. Then, $R_{rws} = 0.596$, which is quite low compared to 0.852. Besides, pole-zero separation is not as critical as before. In addition, to see the performance improvement over the mass–spring chains and DVA equipped spring isolation systems, please compare Figs. 11 and 12 with Fig. 3, which was also generated for the case of $\mu = 0.1$.

Now, let us investigate the effect of $\mu$. In order to make comparisons with the first example shown in Fig. 11, let us keep $T_0 = 0.1$ and increase $\mu$ to 0.5. Then, for the Type II isolator, $m_{is} = 0.5$ and $\alpha = 1.284$. For the

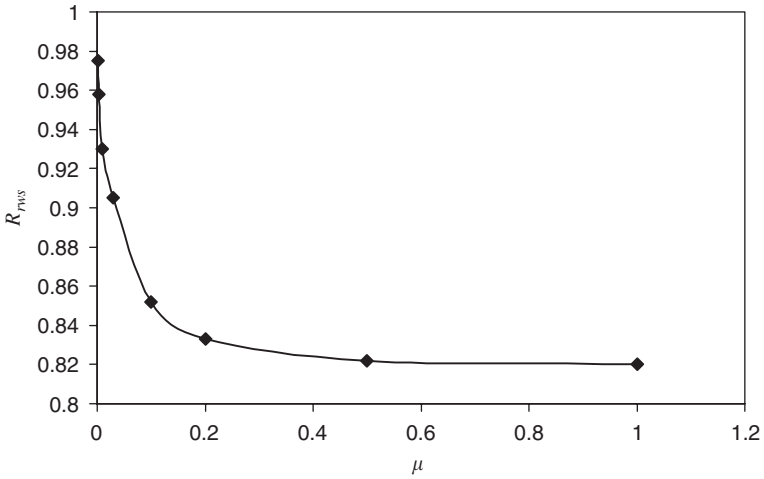


Fig. 14. Graph representing $R_{rws}$ versus $\mu$ for $T_0 = 0.1$.

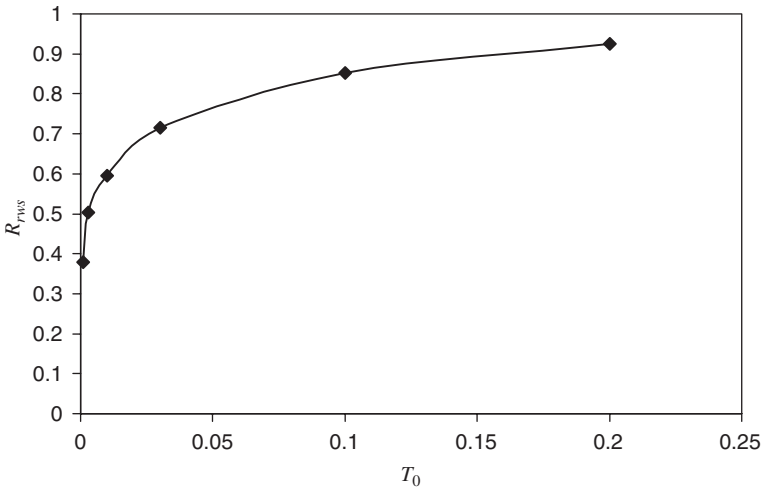


Fig. 15. Graph representing $R_{rws}$ versus $T_0$ for $\mu = 0.1$.

2-dof optimum design, here are the values of the variables: $m_1 = 0.356$, $m_2 = 0.144$, $k_1 = 6.755$, $k_2 = 1.174$, $\alpha_1 = 3.537$, $\alpha_2 = 1.800$. Fig. 13 shows the transmissibility plots of the two systems.

In this case, the normalized stop-band frequency of the Type II isolator can be found to be 1.74. Moreover, normalized stop-band frequency of the 2-dof quasi-optimal design is calculated as 1.43. Then, $R_{rws} = 0.822$, which is little bit less than 0.852. So, there is only slight increase in relative performance of the 2-dof system due to a substantial increase in isolator mass. There is also some increase in the pole-zero separation, but not as much as the case of $\mu = 0.1$ and $T_0 = 0.01$.

The two systems can be compared for other values of $\mu$ and $T_0$. Figs. 14 and 15 show the effect of each parameter on $R_{rws}$. In each graph, only one parameter is changed at a time.

It can be inferred from Fig. 14 that as $\mu$ decreases, the relative performance of the sdof system increases, and as $\mu$ increases, the two systems' relative performance converges to a fixed ratio. Fig. 15 displays the expected dependence of transmissibility on the degree-of-freedom. At low transmissibility values the 2-dof system has substantially better performance.

## 4. Conclusion

In this paper, stop-band frequencies of various low-pass filter-type vibration isolators are formulated using two non-dimensional numbers. It has been shown that to achieve low stop-band frequencies, the isolator mass should not be distributed over the spring that supports the load as in the mass–spring chains, instead all the isolator mass should be utilized to generate anti-resonance frequencies. Two new $n$-dof isolator designs are introduced having this property.

The first design has $n-1$ zeros, which are generated by $n-1$ sdof dynamic vibration absorbers (DVAs). Hence, the isolator mass is distributed among the absorbers. It has been proven that this system has a lower stop-band frequency than an equivalent resonance-only mass–spring chain. The second design is synthesized using lever-type anti-resonant vibration isolators. The order of the pivot points plays an important role in the dynamics of lever-type anti-resonant vibration isolators. So, according to the order of their pivot points they are categorized as Type I and Type II anti-resonant vibration isolators. Based on the stop-band frequency formulations, Type II anti-resonant vibration isolators offer the lowest stop-band frequency among the sdof systems. So, an $n$-dof isolator is synthesized using $n$ Type II isolators in series. In this $n$ stage system, there are $n$ zeros and all of the isolator mass is concentrated on the lever tips to obtain the lowest stop-band frequency in the optimization routine. Finally, the advantage of having multiple stages in lever-type anti-resonant vibration isolators is demonstrated via parametric studies for the case of two stages.

## References

[1] C.E. Crede, *Vibration and Shock Isolation*, Wiley, New York, 1951.
[2] J. Winterflood, High Performance Vibration Isolation for Gravitational Wave Detection, PhD Thesis, The University of Western Australia, 2001.
[3] J. Giaime, P. Saha, D. Shoemaker, L. Sievers, A passive vibration isolation stack for LIGO: design, modeling, and testing, *Review of Scientific Instruments* 67 (1) (1996) 208–214.
[4] L. Brillouin, *Wave Propagation in Periodic Structures: Electric Filters and Crystal Lattices*, McGraw-Hill, New York, 1946.
[5] M.G. Ellis, *Electronic Filter Analysis and Synthesis*, Artech House, Boston, 1994.
[6] S. Niewiadomski, *Filter Handbook: A Practical Design Guide*, Heinemann Newnes, Oxford, 1989.
[7] H. Frahm, Device for damping vibrations of bodies, U.S. Patent No. 989,958, 1911.
[8] C.M. Harris, A.G. Piersol, *Harris' Shock and Vibration Handbook*, McGraw-Hill, New York, 2002.
[9] M.L. Munjal, A rational synthesis of vibration isolators, *Journal of Sound and Vibration* 39 (2) (1975) 247–263.
[10] J.T. Szefi, Helicopter Gearbox Isolation Using Periodically Layered Fluidic Isolators, PhD Thesis, The Pennsylvania State University, 2003.
[11] W.G. Flannelly, Dynamic antiresonant vibration isolator, U.S. Patent No. 3,322,379, 1967.
[12] A.D. Rita, J.H. McGarvey, R. Jones, Helicopter rotor isolation evaluation utilizing the dynamic antiresonant vibration isolator, *Journal of the American Helicopter Society* 23 (1) (1978) 22–29.
[13] D. Braun, Development of antiresonance force isolators for helicopter vibration reduction, *Journal of the American Helicopter Society* 27 (4) (1982) 37–44.
[14] D. Braun, Vibration isolator particularly of the antiresonance force type, U.S. Patent No. 4,781,363, 1988.
[15] R.A. Desjardins, Vibration isolation system, U.S. Patent No. 4,140,028, 1979.
[16] R.A. Desjardins, W.E. Hooper, Antiresonant rotor isolation for vibration reduction, *Journal of the American Helicopter Society* 25 (3) (1980) 46–55.
[17] V.A. Ivovich, M.K. Savovich, Isolation of floor machines by lever-type inertial vibration corrector, *Proceedings of the Institution of Civil Engineers: Structures and Buildings* 146 (4) (2001) 391–402.
[18] E.I. Rivin, *Passive Vibration Isolation*, ASME Press, New York, 2003.
[19] A.J.H. Goodwin, Vibration isolators, U.S. Patent No. 3,202,388, 1965.
[20] D.R. Halwes, Vibration suppression system, U.S. Patent No. 4,236,607, 1980.
[21] M.R. Smith, W.S. Redinger, The model 427 pylon isolation system, *American Helicopter Society 55th Annual Forum*, Montreal, Canada, May 1999.
[22] D.P. McGuire, High stiffness (''rigid'') helicopter pylon vibration isolation systems, *American Helicopter Society 59th Annual Forum*, Phoenix, Arizona, May 2003.
[23] P.E. Corcoran, G.E. Ticks, Hydraulic engine mount characteristics, SAE Paper # 840407, 1984.
[24] W.C. Flower, Understanding hydraulic mounts for improved vehicle noise, vibration and ride qualities, SAE Paper # 850975, 1985.
[25] H.F. Olson, *Dynamical Analogies*, D. Van Nostrand, New York, 1943.